JOURNAL OF MATERIALS SCIENCE 31 (1996) 2951–2956

Crystallization kinetics of amorphous $Pb(Fe_{2/3}W_{1/3})O_3$

NAM-KYOUNG KIM
Department of Inorganic Materials Engineering, Kyungpook National University, Taegu 702-701, Korea

D. A. PAYNE
Department of Materials Science and Engineering and Materials Research Laboratory, University of Illinois at Urbana–Champaign, Urbana, Illinois 61801, USA

Kinetic data analyses on the crystallization behaviour of amorphous lead iron tungstate (PFW) were carried out. A low value of the glass transition/melting point ratio (0.52) and a high value of the frequency factor ($2 \times 10^{37}\ s^{-1}$) of the first crystallization exotherm may indicate a high degree of metastability of the prepared PFW in the amorphous state. The Avrami exponent was determined to be ~ 3.0, which suggests a bulk nucleation. The activation energy for crystallization was averaged to be 520 kJ mol^{-1} for the first exotherm. The validity of the estimated values of the Avrami exponent and the activation energy were confirmed by comparing with an independently obtained product of the two parameters.

1. Introduction

Glass formation is a matter of by-passing crystallization [1]. At cooling rates high enough to prevent the structural relaxation phenomena of crystallization, quenching of the melt results in a glass. Thus the prepared amorphous material is at a higher free energy state compared with the corresponding crystalline form and is thermodynamically metastable. On heating, amorphous materials will release their heat of crystallization as the amorphous structure transforms to the lower free energy modification of a crystalline state.

The formation of the perovskite PFW structure from its constituent oxide components consists of a long and complex sequence of intermediate reactions [2, 3]. Similarly the crystallization from an amorphous precursor is not a straightforward development. Metastable crystalline phases are initially formed during the exothermic crystallization reactions and these are subsequently converted to a stable perovskite phase at higher temperatures [4, 5].

Kinetic data analyses are usually utilized in the interpretation of the thermally stimulated process [6]. Two kinds of analysis methods (isothermal and nonisothermal) are frequently used. In the isothermal (or static) method, a specimen is first heated to the temperature of interest and then thermochemical data are collected as a function of elapsed time while a constant temperature is maintained. In the nonisothermal (or dynamic) method, reaction kinetics data are gathered as a function of temperature while the specimen is heated (or cooled) at a constant rate through the temperature range of interest.

In the present report, graphical data analyses on the crystallization kinetics of amorphous lead iron tungstate, $Pb(Fe_{2/3}W_{1/3})O_3$(PFW), were carried out to evaluate the kinetic parameters of the activation energy, frequency factor, and Avrami exponent as well as the enthalpy change of crystallization and also to verify the validity of a two-thirds rule between the glass transition temperature (T_g) and the melting or liquidus temperature (T_m).

2. Kinetic data analysis

The temperature dependence of the rate constant k can be expressed by an Arrhenius-type equation as

$$k = \nu \times \exp(-\Delta E/RT), \quad (1)$$

where ν, ΔE, R, and T are the frequency factor (or pre-exponential factor), crystallization activation energy, universal gas constant, and absolute temperature, respectively. When the sample is heated/cooled at a constant rate α, the temperature at the time t can be given by $T = T_o + \alpha t$, T_o being the initial temperature. The rate constant can then be restated as

$$k(t) = \nu \times \exp[-\Delta E/R(T_o + \alpha t)]. \quad (2)$$

Several approaches have been applied to the determination of the activation energy and frequency factor by graphical methods. The first one, proposed by Kissinger [7, 8] and modified later by Bansal *et al.* [9, 10], is

$$\ln(\alpha/T_P^2) = \ln \nu - \ln(\Delta E/R) - \Delta E/RT_P, \quad (3)$$

where T_P is the peak temperature of the crystallization exotherm. A plot of $\ln(\alpha/T_P^2)$ vs $1/T_P$ obtained at various heating rates would be linear with a slope of $-\Delta E/R$ and an intercept of $[\ln \nu - \ln(\Delta E/R)]$ on

0022–2461

the ordinate. Bansal *et al.* [9] also proposed an alternative method of the form

$$\ln[\alpha/(T_P - T_o)] = \ln \nu - \Delta E/RT_P, \quad (4)$$

where an Arrhenius plot of $\ln[\alpha/(T_P - T_o)]$ would give a similar gradient of $-\Delta E/R$ with an intercept of ln ν. Ozawa [11] proposed a third equation of the form

$$\ln \alpha = constant - \Delta E/RT_P, \quad (5)$$

where ΔE can obtained from an Arrhenius plot of ln α. Thus, there are three methods available for the analysis of the crystallization process.

The Avrami exponent (n) is a dimensionless constant, which is associated with the crystal nucleation mode. For an estimation of the Avrami exponent, Matusita and Sakka [12] proposed a following expression

$$\ln[-\ln(1 - x)] = -n \times \ln \alpha + constant, \quad (6)$$

where x is the volume fraction crystallized. A plot of $\ln[-\ln(1 - x)]$ vs ln α would be a straight line, from which n can be determined. Meanwhile, Augis and Bennett [13] proposed another equation of the form

$$n = [2.5/\Delta T_{FWHM}] \cdot [T_P^2/(\Delta E/R)], \quad (7)$$

where ΔT_{FWHM} is the full width of the crystallization exotherm at a half maximum height.

Piloyan *et al.* [14] proposed an estimation method for determining the activation energy from a single run of differential scanning calorimetry (DSC). The value obtained is actually a product of an Avrami exponent and the activation energy (i.e., $n\Delta E$), this point is discussed by Bansal *et al.* [15] The Piloyan method is expressed as

$$\ln \tilde{x} = constant - n\Delta E/RT, \quad (8)$$

where $\tilde{x}$ is the height of the exotherm measured from the baseline. The product of $n\Delta E$ can then be obtained from the slope of an Arrhenius plot of ln $\tilde{x}$.

3. Experimental procedure

Amorphous PFW was prepared in the form of thin (~ 20 μm) flakes by a twin-roller quenching method at a cooling rate of ~ 10^6 K s^{-1}, details of which were reported previously [4, 16]. Information on the phase development and microstructural evolution during crystallization can be found elsewhere [4, 5]. The flakes were crushed, ground, and the crystallization behaviour was investigated by thermochemical techniques using a DSC interfaced with a computerized data acquisition and manipulation system. A series of nonisothermal DSC runs were carried out over a range of heating rates (2.5–80 °C min^{-1}) in order to collect crystallization information. In addition, isothermal DSC runs were also tried to allow comparison of the results. All of the DSC runs were performed under flowing oxygen. Analysis of the gathered kinetic data were performed, using the various procedures described in section 2, thus allowing insights into the crystallization behaviour.

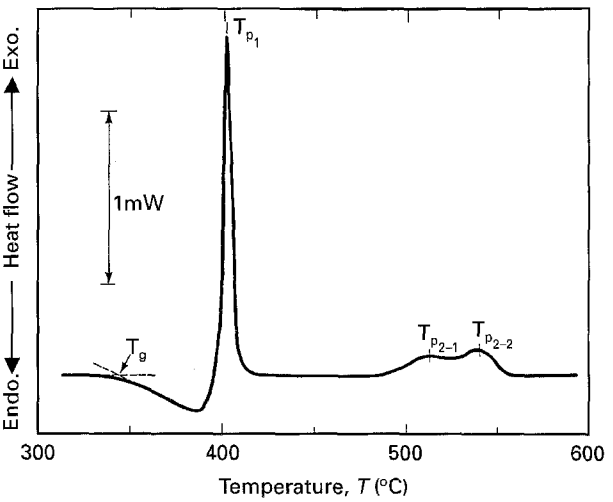

Figure 1 DSC thermogram of as-quenched PFW.

4. Results and discussion

A typical DSC result (α = 10 °C min^{-1}) is given in Fig. 1. Transition temperatures were read to the nearest 5 °C, at the extrapolated onset point for each peak. The specimen underwent the broad endothermic reaction of glass transition starting at 350 °C, followed by the sharp exotherm of crystallization at 395 °C. The two broad exothermic peaks around 500–550 °C range were not clearly resolved and hence will hereafter be treated as one exotherm.

For ordinary glasses containing network-forming cations, the ratio of the glass transition temperature (T_g) to the melting or liquidus temperature (T_m) is typically 2/3 and is called the two-thirds rule [17, 18], where temperatures are in absolute degrees. Nassau *et al.* prepared quenched glasses in the system Li_2O–RO_3 (R = W, Mo) [19], $La_2(SO_4)_3 - Li_2SO_4$ [20], and three compositions (2212, 4334, and 2223) of the (Bi, Sr, Ca, Cu)O_x superconductor [21]. Using their data, the calculated T_g/T_m ratios fell in the range 0.60–0.68 and closely followed the rule. Tatsumisago *et al.* [22] prepared amorphous materials in the system of R_2O–WO_3 (R = Li, Na, K) and reported the ratios of 0.58–0.68, which also approximate to the rule. On the other hand, significant deviations (with ratios of 0.47–0.54) for glasses of $70Li_3BO_3 \cdot 30(Li_4GeO_4$, Li_4SiO_4, Li_3PO_4, Li_2WO_4, and $Li_2SO_4)$ produced by the twin-roller quenching method have been reported [23]. Other cases of violation include quenched glasses of Li_2O–SiO_2 (T_g[24], (T_m[25]) and quenched $KF \cdot LiF \cdot Al_2O_3 \cdot 3SiO_2$ [26] with calculated ratios of 0.44–0.51 and 0.44–0.46, respectively. Of the two compositions of 70 and 83.3 mol % Li_2O in the system Li_2O–Al_2O_3 [27], the first composition observed the rule ($T_g/T_m = 0.62$), whereas the ratio of the second composition was significantly different (0.53).

For amorphous PFW, the glass transition temperature and melting point were 350 and 935 °C [4, 16], respectively. The ratio between the temperatures is 0.52 and this deviates significantly from the two-thirds rule. The reason why some amorphous materials obey the rule and others (including amorphous PFW) do not is currently not clear. However, it is currently

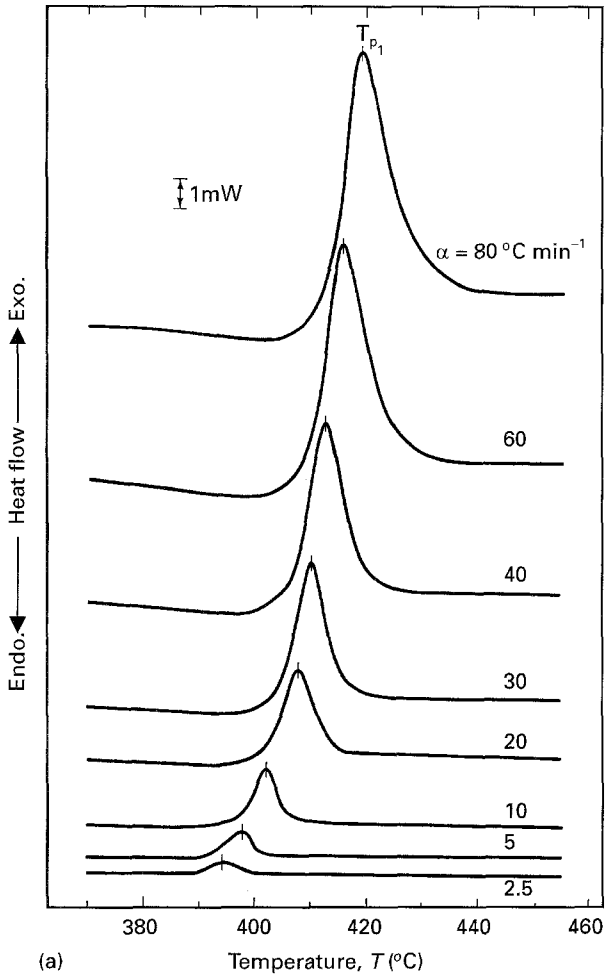

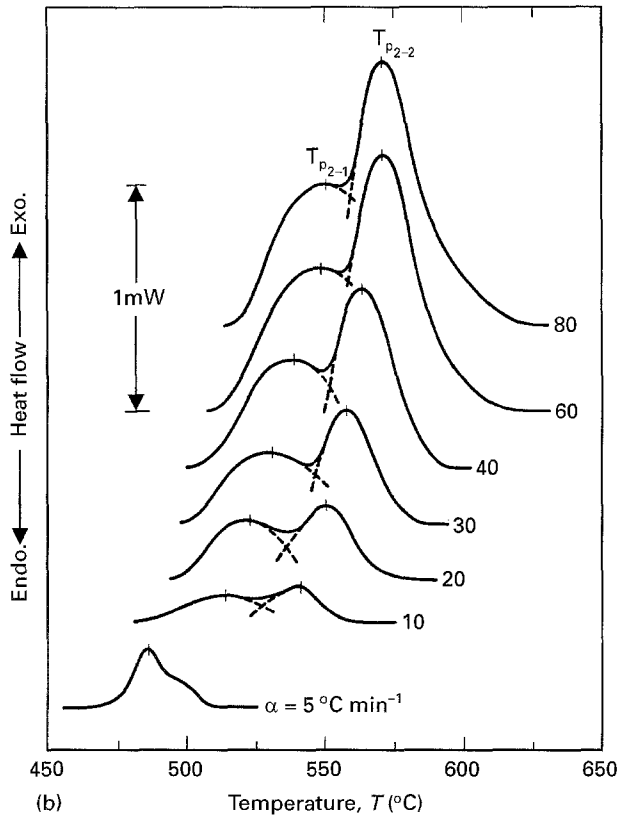

Figure 2 Variations in the (a) first and (b) second crystallization exotherm as a function of heating rates. Note that scales in abscissa and ordinate are different.

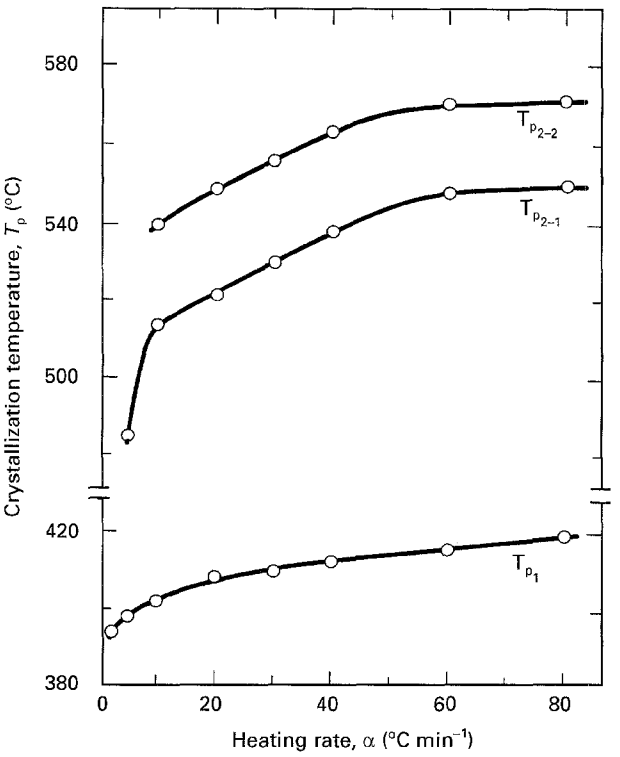

Figure 3 Heating rate dependence of crystallization temperature.

believed to be associated with the chemical composition (e.g., presence of network former ions) as well as the specimen preparation method (e.g., quenching rate), leading to different degrees of metastability.

In order to observe the evolution of the crystallization exotherms, a series of DSC runs (at heating rates of 2.5, 5, 10, 20, 30, 40, 60, and 80 °C min^{-1}) were carried out across the temperature range of the two crystallization exotherms of Fig. 1. Fig. 2 illustrates the effect of the heating rate on the crystallization exotherms, which shift to higher temperatures with an increase in the heating rates. In Fig. 2b, peak height reversal is noticeable at heating rates between 5 and 10 °C min^{-1}. Measured values of the enthalpy change of the two crystallization exotherms were averaged to be 12.7 and 9.5 J g^{-1}, respectively. The peak temperatures of crystallization, denoted by tick marks, are plotted against heating rates (Fig. 3), where the peak temperatures of the first exotherm (T_{P_1}) do not change as much as those of the second exotherm ($T_{P_{2-1}}$ and $T_{P_{2-2}}$ of two sub-peaks).

The volume fraction crystallized (x) was estimated from the ratio between the partial area of the exotherm up to the temperature and the total area of the exotherm above the baseline [28, 29]. This concept was applied to the first exotherm and the results are illustrated in Fig. 4, where values of x at the peak temperature (x_P) are marked by open circles. The value of x decreased gradually with increasing heating rates, with the exception of 2.5 °C min^{-1}, and all of the curves showed the general tendency of a well-developed sigmoidal shape.

Using the procedures outlined in section 2, $\ln[\alpha/T_P^2]$, $\ln[\alpha/(T_P - T_o)]$, and $\ln\alpha$ were plotted against $1/T_P$ for the first crystallization process (Fig. 5) and similar activation energy values of 520, 505, and

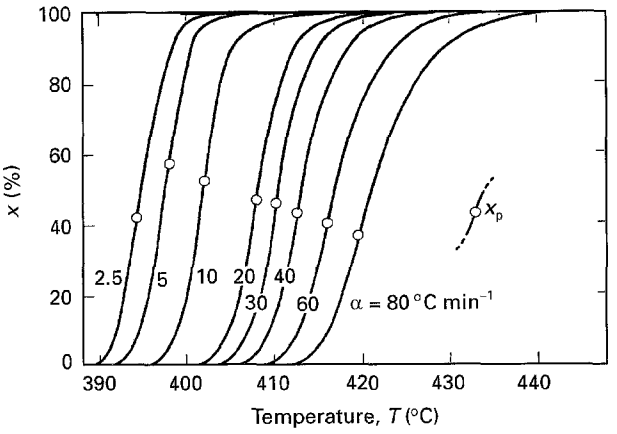

Figure 4 Temperature dependence of crystallized volume fraction of the first exotherm, as a function of heating rates.

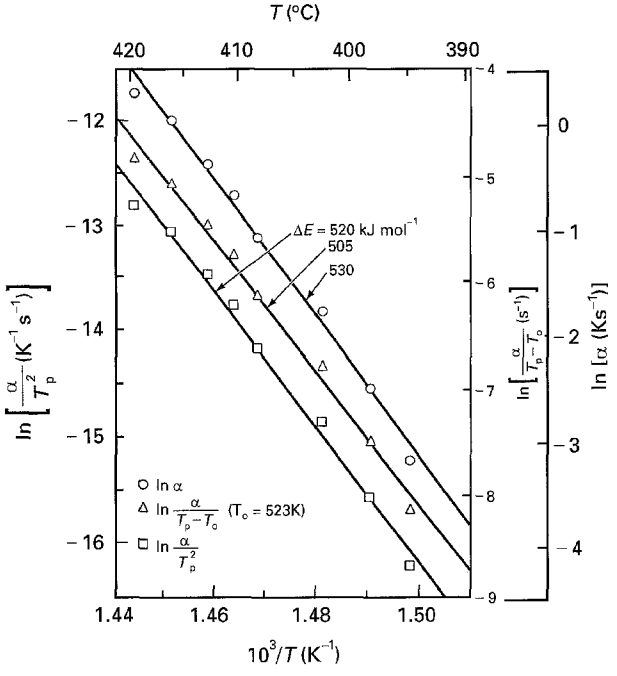

Figure 5 Arrhenius plots of $\ln[\alpha/T_p^2]$, $\ln[\alpha/(T_p - T_o]$, and $\ln \alpha$ of the first crystallization exotherm.

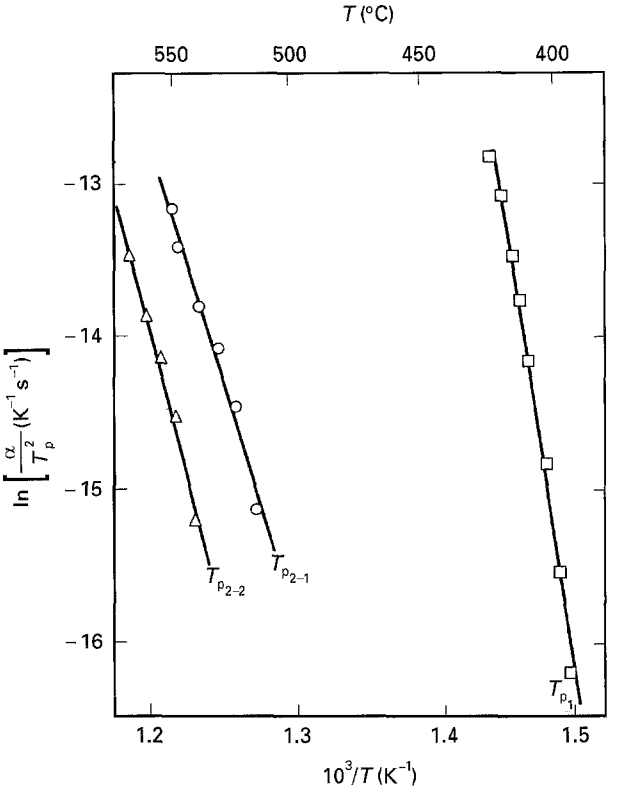

Figure 6 Arrhenius plots of $\ln[\alpha/T_p^2]$ of the three crystallization peaks.

TABLE I Activation energy, frequency factor, and Avrami exponent

	ΔE (kJ mol^{-1})	ν (s^{-1})	n
Peak 1	520[a] 505[b] 530[c] (520)[d]	3×10^{38},[a] 1×10^{36},[b] (2×10^{37})[d]	3.1[e]
Peak 2–1	260 260 270 (260)	3×10^{15} 9×10^{13} (5×10^{14})	
Peak 2–2	310 310 320 (310)	1×10^{18} 3×10^{16} (2×10^{17})	

a: by the Kissinger method of Equation 3
b: by the Bansal method of Equation 4
c: by the Ozawa method of Equation 5
d: average value
e: by the Matusita–Sakka method of Equation 6

530 kJ mol^{-1} were obtained by the three different methods. Fig. 6 illustrates the Arrhenius plots of $\ln[\alpha/T_p^2]$ for the first and second exotherms. By using Equations 3–5, it was possible to obtain the activation energy and frequency factor of the individual crystallization processes and these are listed in Table 1. Average values of the crystallization activation energies were 520, 260, and 310 kJ mol^{-1}, which are equivalent to 5.4, 2.7, and 3.2 eV, respectively. Meanwhile, the crystallization activation energy of amorphous $LiNbO_3$ (prepared by rapid quenching) was reported to be 2.47–2.7 eV [30, 31]. The activation energies of the second exotherm (2.7–3.2 eV) of amorphous PFW fall in the same range as that of $LiNbO_3$ (2.5–2.7 eV), though somewhat higher, while that of the first crystallization process (5.4 eV) is twice as high.

The frequency factors of the two crystallization exotherms were $\sim 10^{37}$ and $\sim 10^{15-17}$ s^{-1}, respectively (Table 1). The value of amorphous $KNbO_3$, prepared by twin-roller quenching, was reported to be $\sim 10^{43}$ s^{-1} for its second crystallization exotherm [32], while those of amorphous $LiNbO_3$ were calculated with reported data [31] by using the Kissinger method (Equation 3) and were $\sim 10^{13}$ and $\sim 10^{14}$ s^{-1} for the two crystallization peaks. Meanwhile, the frequency factors of amorphous $PbTiO_3$ showed a strong dependency on the preparation method: i.e., $\sim 10^{15}$ s^{-1} (by sol–gel method), $\sim 10^{18}$ s^{-1} (by coprecipitation), and $\sim 10^{37}$ s^{-1} (by rapid solidification using the twin-roller quenching technique) [33]. Among these, amorphous PFW (first exotherm), amorphous $KNbO_3$ (second exotherm), and amorphous $PbTiO_3$ (prepared by rapid solidification) show unusually high values of the frequency factor. Such high values seem to be an indication of the high degree of metastability and may probably be related to the instantaneous crystallization tendency of amorphous

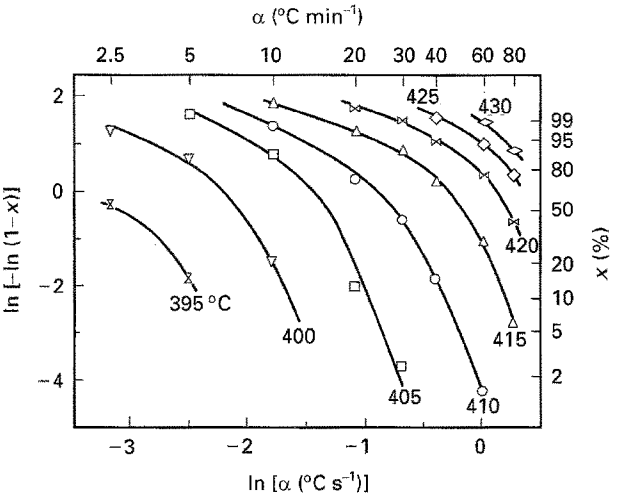

Figure 7 Matusita–Sakka plot of $\ln[-\ln(1-x)]$ vs $\ln\alpha$ at different temperatures.

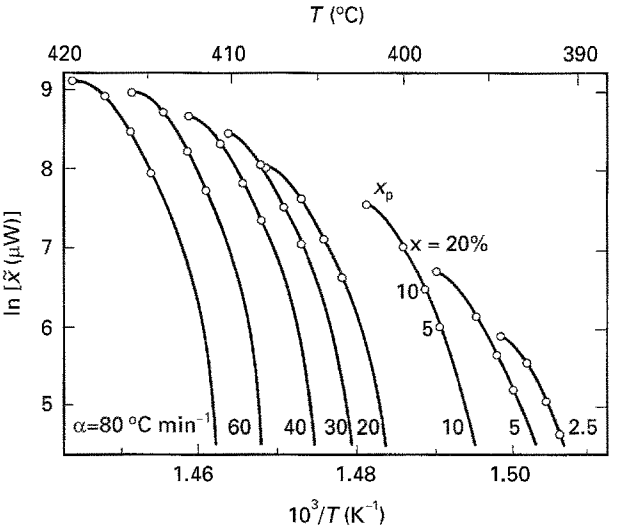

Figure 8 Piloyan plot of $\ln\tilde{x}$ vs $1/T$ at different heating rates.

TABLE II Kinetic parameters of the first crystallization exotherm

α (°C min^{-1})	ΔT_{FWHM}[a] (°C)	n[b]	$n\Delta E$[c] (kJ mol^{-1})
2.5	5.7	3.1	1820
5	4.9	3.6	1600
10	4.6	3.9	1720
20	6.0	3.0	1630
30	5.7	3.2	1640
40	6.5	2.8	1550
60	7.5	2.5	1500
80	8.9	2.1	1330
Average		3.0	1600

a: read from Fig. 2a.
b: by the Augis–Bennett method of Equation 7.
c: by the Piloyan method of Equation 8.

PFW on heating, which can be observed in Fig. 3 where a small temperature shift (~ 25 °C) in the first exotherm with increasing heating rate can be seen.

A Matusita–Sakka plot of $\ln[-\ln(1-x)]$ vs $\ln\alpha$ is given in Fig. 7, where the plots are nonlinear, as opposed to the authors' claim of linearity of Equation 6. However, their plots [12, 34] were not straight either, so the validity of Equation 6 might need to be reexamined. Due to the curvature of Fig. 7, values of the slope depend on the position of the measurement. By considering the validity of Equation 8 in the range of $x \leqslant 0.2$ [15], the lower part of the curves seems more suited for the estimation of the Avrami exponent. The results obtained are: 2.2 (395 °C), 2.6 (400), 3.1 (405), 3.2 (410), 3.0 (415), 2.3 (420), 1.6 (425), and 1.3 (430). Amongst these values, only the three (3.1, 3.2, and 3.0 at 405, 410, and 415 °C, respectively) satisfy the requirement ($x \leqslant 20\%$) and the Avrami exponent was taken as a mean value of 3.1 (Table 1).

The widths of the exotherm at a half maximum (ΔT_{FWHM}) of the first crystallization process, obtained from the DSC data of Fig. 2a, are listed in Table II. The Avrami exponents were determined by using the Augis–Bennett method of Equation 7 and are also listed. The average value of the Avrami exponent is 3.0 and is in good agreement with the 3.1 obtained by the Matusita–Sakka method in the previous paragraph. An Avrami exponent of ~ 3.0 suggests bulk nucleation within the amorphous matrix on crystallization, which was confirmed in the microstructure observation [4, 5].

A Piloyan plot is given in Fig. 8 for the values of $\tilde{x}$ up to the peak temperature. Due to the validity of Equation 8 at $x \leqslant 0.2$, slopes were read as the average value in the range of $5 \leqslant x \leqslant 20\%$ and $n\Delta E$ products obtained from the slopes are listed in Table II. Since both the activation energy (520 kJ mol^{-1}) and the Avrami exponent (3.1 by Matusita–Sakka method and 3.0 by Augis–Bennett method) were previously obtained independently, their validity can now be checked by the result of the Piloyan method. The product of $n\Delta E$ is 1560 or 1610 kJ mol^{-1} (depending on the method of the Avrami exponent determination) and is in excellent agreement with the independent data of 1600 kJ mol^{-1} obtained by the Piloyan method. Hence, the appropriateness of the determined values of the Avrami exponent and the activation energy was confirmed.

Isothermal DSC runs were tried at the temperature of the first crystallization exotherm. After the scan, the specimen was tested again using nonisothermal DSC to check if any crystallization reactions had occurred during the isothermal run. For isothermal conditions up to 370 °C, no crystallization was detected. Above 380 °C, however, isothermal crystallization was so rapid (< 20 s) that it was almost impossible to distinguish the crystallization exotherm from the initial temperature rise (caused by a momentary temperature overshoot in the equipment). The instantaneous crystallization behaviour, which made the isothermal run very difficult, is currently believed to be due to the high degree of metastability inherent to the amorphous PFW. An extremely high quenching rate, as mentioned previously, is necessary to prepare PFW in the amorphous state without any help of network-forming cations, and this might have introduced an appreciable degree of metastability to the structure.

5. Summary

An amorphous PFW specimen was examined by using nonisothermal DSC techniques. The calculated ratio between the glass transition temperature and the melting point was 0.52, which was significantly different from the two-thirds rule. Kinetic data analyses on the crystallization behaviour were performed. The enthalpy changes of crystallization were averaged to be 12.7 and 9.5 $J g^{-1}$ for the two exotherms. Through the use of Kissinger, Bansal, and Ozawa plots, the activation energy and frequency factor were determined to be 520 $kJ mol^{-1}$ and $2 \times 10^{37} s^{-1}$ for the first exotherm, and 260–310 $kJ mol^{-1}$ and $10^{15-17} s^{-1}$ for the second exotherm of the two sub-peaks. The unusually high value of frequency factor of the first stage of crystallization may indicate a highly metastable state of the amorphous PFW.

Through the use of the Matusita–Sakka method the Avrami exponent was determined to be 3.1, as compared with a value of 3.0 which was obtained by the Augis–Bennett method. The behaviour of the bulk nucleation, observed in the microstructural development, supported the validity of calculated value of ~ 3.0. The value of $n\Delta E$ was determined to be 1600 $kJ mol^{-1}$ from the Piloyan method whilst 1560–1610 $kJ mol^{-1}$ was obtained from the independently determined Avrami exponent and activation energy. The excellent agreement between them confirmed the validity of the Avrami exponent and the activation energy, obtained in the current study.

References

1. D.TURNBULL, *Contemp. Phys.* **10** (1969) 473.
2. M. P. KASSARJIAN, R. E. NEWNHAM and J. V. BIGGERS, *Amer Ceram. Soc. Bull.* **64** (1985) 1108.
3. M. YONEZAWA and T. OHNO, Proceedings of the Japan-US Study Seminar on Dielectric and Piezoelectric Ceramics (1982) p. T-8.
4. N. K. KIM, Ph. D. Thesis, University of Illinois at Urbana-Champaign, Urbana, Illinois, 1988.
5. N. K. KIM and D. A. PAYNE, *Kor. J. Ceram.* **1** (1995) 75.
6. R. CHEN and Y. KIRSH, "Analysis of Thermally Stimulated Processes" (Pergamon Press, Oxford, 1981).
7. H. E. KISSINGER, *J. Res. NBS.* **57** (1956) 217.
8. *Idem, Anal. Chem.* **29** (1957) 1702.
9. N. P. BANSAL, R. H. DOREMUS, A. J. BRUCE and C. T. MOYNIHAN, *J. Amer. Ceram. Soc.* **66** (1983) 233.
10. N. P. BANSAL and R. H. DOREMUS, *J. Therm. Anal.* **29** (1984) 115.
11. T. OZAWA, *Ibid.* **2** (1970) 301.
12. K. MATUSITA and S. SAKKA, *Phys. Chem. Glasses* **20** (1979) 81.
13. J. A. AUGIS and J. E. BENNETT, *J. Therm. Anal.* **13** (1978) 283.
14. G. O. PILOYAN, I. D. RYABCHIKOV and O. S. NOVIKOVA, *Nature* **212** (1966) 1229.
15. N. P. BANSAL, A. J. BRUCE, R. H. DOREMUS and C. T. MOYNIHAN, *J. Non-Cryst. Solids* **70** (1985) 379.
16. N. K. KIM and D. A. PAYNE, *J. Mater. Res.* **5** (1990) 2045.
17. S. SAKKA and J. D. MacKENZIE, *J. Non-Cryst. Solids* **6** (1971) 145.
18. H. KANNO, *ibid.* **44** (1981) 409.
19. K. NASSAU, A. M. GLASS, M. GRASSO and D. H. OLSON, *J. Electorochem. Soc.* **127** (1980) 2743.
20. K. NASSAU and A. M. GLASS, *J. Non-Cryst. Solids* **44** (1981) 97.
21. K. NASSAU, A. MILLER, E. M. GYORGY and T. SIEGRIST, *J. Mater. Res.* **4** (1989) 1330.
22. M. TATSUMISAGO, I. SAKONO, T. MINAMI and M. TANAKA, *J. Mater. Sci.* **17** (1982) 3593.
23. M. TATSUMISAGO, H. NARITA, T. MINAMI and M. TANAKA, *J. Amer. Ceram. Soc.* **66** (1983) C210.
24. M. TATSUMISAGO, T. MINAMI, and M. TANAKA, *ibid.* **64** (1981) C97.
25. E. M. LEVIN, C. R. ROBBINS and H. F. McMURDIE, "Phase Diagrams for Ceramists, 2nd edn." (American Ceramic Society, Columbus, Ohio, 1969) Figs 182–184.
26. S. KAWAI and M. MOTOYAMA, *Yogyo-Kyokai-Shi* **98** (1990) 604.
27. K. NASSAU, M. GRASSO and A. M. GLASS, *J. Non-Cryst. Solids* **34** (1979) 425.
28. H. J. BORCHARDT and F. DANIELS, *J. Amer Chem. Soc.* **79** (1957) 41.
29. F. SKVARA and V. SATAVA, *J. Therm. Anal.* **2** (1970) 325.
30. K. NASSAU, *J. Non-Cryst. Solids* **42** (1980) 423.
31. M. MAEDA, T. KUBO, H. SATO and T. IKEDA, *Jpn. J. Appl. Phys.* **22–2** (1983) 25.
32. L. DROZDYK, private communication.
33. R. W. SCHWARTZ and D. A. PAYNE, "Better Ceramics Through Chemistry III" edited by C. J. Brinker, D. E. Clark, and D. R. Ulrich (Materials Research Society, 1988) p. 199.
34. K. MATUSITA and S. SAKKA, *Thermochim. Acta* **33** (1979) 351.

Received 6 March
and accepted 1 December 1995